The Gulf Stream—Barrier or Blender?

A. S. BOWER, H. T. ROSSBY AND J. L. LILLIBRIDGE

Graduate School of Oceanography, University of Rhode Island, Kingston, RI 02881

(Manuscript received 9 November 1983, in final form 3 August 1984)

ABSTRACT

The Gulf Stream '60 hydrographic survey has been used to examine the distribution of water properties across the Gulf Stream as a function of potential density. This survey covered a half million square miles of Slope, Gulf Stream and Sargasso Sea Waters in the western North Atlantic. Quantities plotted as a function of density are acceleration potential, potential temperature, dissolved oxygen and potential vorticity.

The transition from Sargasso Sea Water to Slope Water in the upper thermocline ($\sigma_\theta < 27.1$) is sharp and coincides closely with the dynamical boundary of the Gulf Stream, defined by the gradient of acceleration potential. This indicates that water mass exchanges across the Gulf Stream–Slope Water front are limited at these levels. Below the 27.1 σ_θ surface, the gradient of acceleration potential still reveals the position of the Stream, but there is no coincident water mass boundary. This and the uniformity of potential vorticity across the Stream suggest that the deep property fields are being efficiently homogenized by mesoscale exchanges across the Gulf Stream. A cross-frontal eddy diffusivity of $K_H = 2.5 \times 10^6$ cm^2 s^{-1} estimated from oxygen flux calculations agrees well with previously published values for frontal regimes.

1. Introduction

In preparation for Lagrangian studies of fluid motion in the Gulf Stream using a new class of isopycnal floats, we thought it would be instructive to use the Gulf Stream '60 (GS '60) hydrographic survey (Fuglister, 1963) to prepare a set of sections of water properties as a function of potential density spanning the Gulf Stream region east of 70°W. Specifically, we sought evidence of the extent to which the Gulf Stream acts as a barrier, isolating the Slope Waters from the Sargasso Sea on the one hand, and serving to stir and mix these waters on the other. Our interest was prompted by recent direct observations of fluid motion as revealed by the trajectories of several Sofar floats. Although these floats are isobaric devices, at 700 m they showed a strong tendency to remain trapped in the Stream, whereas deep floats often seemed to cross the path of the Stream as if it were transparent. These are discussed in detail by Shaw and Rossby (1984). What intrigues us here is that little attention seems to have been given to the consequences of stirring and mixing of the waters in and around the Gulf Stream.

The early literature on the Gulf Stream pictured it as a highly stirred system. Rossby (1936) modeled it as a free turbulent jet increasing its transport downstream by turbulent entrainment from both sides. As evidence of lateral mixing he showed how the core of low-oxygen waters (σ_θ = 27.2) is lost as it is advected northward from the Gulf of Mexico. He also speculated on specific pathways by which waters from the Sargasso Sea could be transferred across the Stream into the Slope Waters. (The turbulent jet concept has not been given much attention since then.)

The very large horizontal eddy viscosity (10^8 cm^2 s^{-1}) which Munk (1950) employed to model the Gulf Stream in his ocean circulation study implies vigorous lateral mixing even though he was not concerned with mixing per se. Stommel (1965) pointed out that this extremely large value could only apply to the climatological mean Gulf Stream, and not to the instantaneous Stream itself. Thus, it is important to distinguish between the properties of the Gulf Stream itself and its domain of influence through meandering. Yet, in virtually all maps of eddy potential and kinetic energy, the Gulf Stream as we know it is replaced by a broad energetic region of great eddy energy, giving the impression of a vigorously stirred system.

In more recent years the ideas of a viscous Stream have given way to that of a much more discrete system with strong local dynamical constraints. Where the Gulf Stream parts from the coast at Cape Hatteras, it becomes a free baroclinic jet. Unbounded both laterally and vertically, it "wiggles" about in increasingly large meanders such that by 65°W, 1000 km east of Cape Hatteras, the meandering envelope is nearly 500 km wide. Yet, except at those moments when rings are being "pinched" off, there is every indication that the Stream is a simply connected, ~100 km wide current as far east as 50°W, a distance well over 2000 km. Even though there is tremendous horizontal shear on both sides of the Stream, as well

as vertical shear, the current maintains structural integrity.

It is the shoaling of the main thermocline along the Gulf Stream that provides the baroclinic pressure field to balance the increasing transport. Fofonoff (1962) and Veronis (1973) have argued that it is this upper bound on the baroclinicity that forces the Gulf Stream to separate from the coast. Viewed this way, the surface front is simply the main thermocline placed on edge. Consequently, there should be no extension of isopycnal surfaces across the front. Thus, besides being a baroclinic jet, the Gulf Stream must also be a material boundary between water masses in the absence of cross-isopycnal mixing. Without cross-boundary advection or mixing, there should be a strong tendency for fluid parcels in the Stream to remain south of the frontal zone. (In reality the isopycnal surfaces do extend north of the Stream as a shallow pycnocline which is subject to seasonal change by the atmosphere.)

In this paper, we want to emphasize the synoptic evidence for these competing characteristics of the Stream; the cross-boundary exchange versus the impermeability of the Stream front itself. In what regions does the Stream separate the waters to either side of it? Does the barrier break down east of 65°W where the meander envelope enlarges? When a "property front" can be identified, does it always coincide with the dynamical front or can local time dependence force a divergence of the two? Using the GS '60 hydrographic survey, which is truly remarkable for its quality and coverage, we have prepared a series of hydrographic sections with potential density as the ordinate rather than pressure. The following quantities are plotted in section form:

1) acceleration potential,
2) potential temperature,
3) dissolved oxygen and
4) potential vorticity.

In addition, pressure, acceleration potential, and oxygen have been plotted in plan view on the $26.8\sigma_\theta$ surface to make estimates of the cross-stream exchanges using a simple box model.

In Section 2, we describe the methods used to construct the sections and isopycnal maps. This is followed by a discussion of the major features in the hydrographic sections in Section 3. In Section 4 we use a simple box model to estimate the permeability of the Gulf Stream. The results are summarized in Section 5.

2. Procedures

The sections and isopycnal maps were constructed using hydrographic data from the GS '60 survey. Only the nine meridional sections completed during the first phase of the survey are included in our study (Fuglister, 1963). These nine sections cover the Slope, Gulf Stream and Sargasso Sea Water regions between 68 and 52°W, extending from the shelf break south of Nova Scotia and Newfoundland to the latitude of Bermuda. The bathymetry is relatively flat, with the exception of the New England Seamounts which form a NW–SE diagonal centered at 60°W.

Standard depth data from this survey were interpolated linearly to obtain values at 0.05 sigma-theta intervals. Then potential temperature, oxygen, acceleration potential and potential vorticity were replotted in section form as a function of potential density between $\sigma_\theta = 26.6$ and $\sigma_\theta = 27.85$. Contours were drawn using a computer plotting package. Results from only four of the nine GS '60 sections are presented in this portion of the study: Sections I and III from west of 60°W and Sections VII and VIII representing the region east of 60°W.

The plan view maps of pressure, acceleration potential and oxygen on the potential density surface $\sigma_\theta = 26.8$ were plotted using all nine sections from GS '60. Contours for these figures were drawn by hand using Fuglister's (1963) Fig. 5 (200 m temperature) as a guide to the position of the Stream path.

Data from the GS '60 survey are generally of good quality. However, Fuglister (1963) does mention that oxygen data from the upper 1500 m in Sections IV, V and VI are biased low. These three sections are included only in the isopycnal maps, so the reader is cautioned that the contours of oxygen may be somewhat uncertain near these sections.

Acceleration potential was calculated, using the method first described by Montgomery (1937), to give an indication of the geostrophic velocity field in the region. (Others who have used variations of this method are Reid, 1965; Tsuchiya, 1968; and Buscaglia, 1971.) Usually, the dynamic height gradient along a pressure surface is used to compute geostrophic velocities relative to some reference pressure surface. The analogous quantity in isopycnal coordinates is acceleration potential. The density surface, $\sigma_\theta = 27.85$, was chosen as the reference level based on the results of an integral divergence test performed on the GS '60 hydrographic data (Barba, 1978). This surface is about 2500 m deep in the Slope Water and 2700 m deep south of the Gulf Stream. Some of the northern stations are in water shallower than 2500 m, so no acceleration potential calculation was attempted for these stations.

For a continuously stratified fluid, the potential vorticity is given by $(f + \xi) \times E$, where f is the Coriolis parameter, ξ the relative vorticity, and E is the static stability, defined by $E = -\rho^{-1}\partial\rho/\partial z$. Due to the lack of stations directly in the Gulf Stream, the relative vorticity cannot be estimated, so we approximate the potential vorticity as simply $f \times E$, which is an accurate measure of the total potential vorticity everywhere except in the regions of large lateral shear in the Gulf Stream. Even in the deep

Gulf Stream ($z \sim 1000$ m), the relative vorticity is small ($\xi \sim 0.05f$) so $f \times E$ is a good approximation to the total potential vorticity. For these calculations, the stability can be rewritten as $E = g\Delta\sigma_\theta/\Delta p$. We took the pressure difference between surfaces separated by 0.10 sigma units to plot potential vorticity as a function of potential density.

3. The sections

a. *Section I*

Section I, the most westerly of the nine GS '60 hydrographic sections, runs along 68°30'W from 40 to 33°N. The acceleration potential field for this section is shown in Fig. 1a. The reader is reminded here that although the density surfaces appear level in this and the following figures, in fact, all the density surfaces slope downward steeply in the vicinity of the Gulf Stream. In Fig. 1a, this occurs between 38 and 37°N, where, for example, the $26.8\sigma_\theta$ surface deepens from about 100 m in the Slope Water to 700 m in the Sargasso Sea (see Fig. 5).

Contours of acceleration potential are every 1 J kg^{-1} (0.1 dynamic meters). What is most significant in this figure is not the actual shape of the contours, but the gradient of acceleration potential along the density surfaces. The steep gradient between 38 and 37°N indicates where the Gulf Stream crosses Section I (flowing into the page). As we would expect, the gradient of acceleration potential along the shallower density surfaces is larger, indicating higher downstream speeds, while at depth the gradient, and hence the velocity, both decrease. It is important to notice that, while the downstream velocity at depth is quite weak, there is still evidence that such a flow exists as far down as the $27.8\sigma_\theta$ surface.

The temperature field for Section I is shown in Fig. 1b, with contours every 1°C. Here, stippled regions indicate contact with the sea floor, but in later figures, they represent sea surface outcropping as well. A sharp temperature front centered at station 5880 coincides exactly (as near as we can tell) with the highest velocity waters as determined from the gradient of acceleration potential. Along the $26.6\sigma_\theta$ surface, the temperature gradient is strong (6°C difference between stations 5879 and 5881), but the gradient weakens with depth such that below the

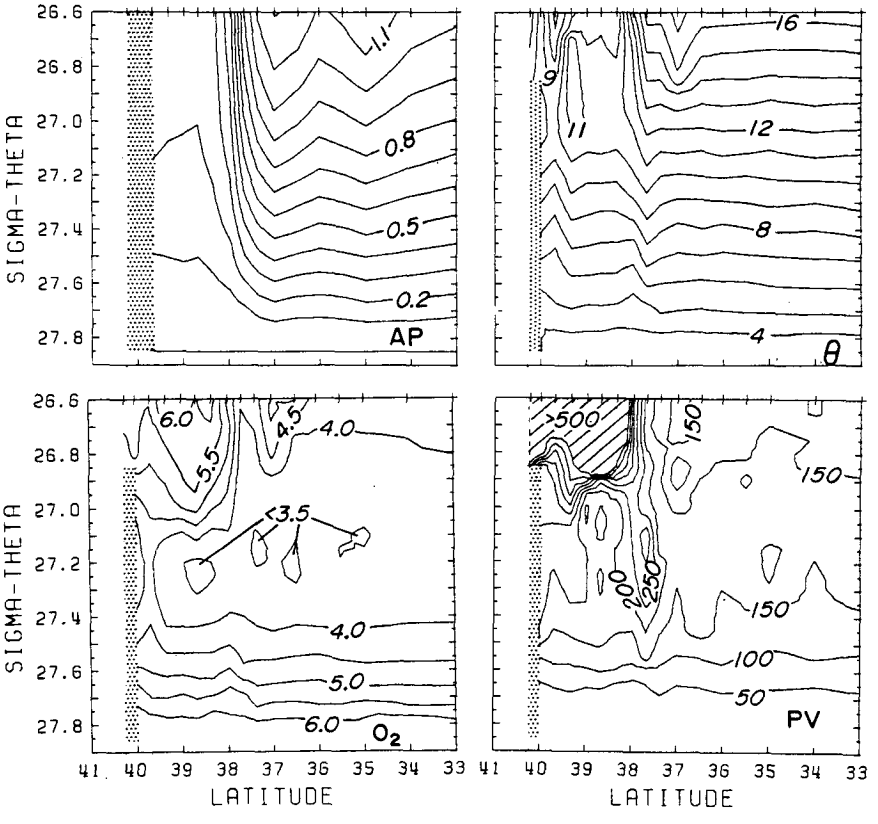

FIG. 1. Property sections for Section I of the GS '60 survey of 68°30'W, R.V. *Atlantis* 255 stations 5873–5889 (N to S): (a) acceleration potential (AP) (dynamic meters) referenced to $\sigma_\theta = 27.85$, (b) potential temperature θ (°C), (c) dissolved oxygen (O_2) (ml l^{-1}), (d) potential vorticity (PV) (see text for definition) (10^{-14} cm^{-1} s^{-1}). Stipple indicates contact with the sea floor or sea surface outcropping. Cross-hatch indicates PV > 500×10^{-14} cm^{-1} s^{-1}.

$27.1\sigma_\theta$ surface, there is only a 1°C difference across the Stream.

North of the Stream, the temperature distribution is patchy but one can see cold, fresh Shelf Water north of station 5876 and above the $26.9\sigma_\theta$ surface. South of the Gulf Stream, the isotherms are quite level, indicating a relatively constant T–S relationship for these waters. The slight downward slope of the isotherms between 10 and 5°C may indicate the influence of more salty Mediterranean Water.

Figure 1c shows the oxygen distribution for this section as a function of density. The contour interval is 0.5 ml l^{-1}. Although dissolved oxygen is a primary constituent in biological processes, on short time scales (months) it can be considered a conservative tracer. In our later discussion concerning the oxygen budget we will estimate the effects of biological processes, and demonstrate their relative insignificance.

Between the 26.6 and $27.1\sigma_\theta$ surfaces, there is a strong cross-stream oxygen gradient associated with the Gulf Stream. On the $26.7\sigma_\theta$ surface, oxygen values decrease from 6.0 to 4.0 ml l^{-1} across the Stream. But below the $27.1\sigma_\theta$ surface, the cross-stream oxygen distribution is quite uniform. A similar picture emerges from the potential vorticity distribution (Fig. 1d). Contour intervals here are every 50×10^{-14} cm^{-1} s^{-1} between 0 and 500×10^{-14} cm^{-1} s^{-1}, and regions with values greater than 500×10^{-14} cm^{-1} s^{-1} are hatched. Shallower than the $27.0\sigma_\theta$ surface, there is a huge difference in potential vorcity across the Stream, from 150×10^{-14} cm^{-1} s^{-1} to greater than 500×10^{-14} cm^{-1} s^{-1}.

Below the $27.0\sigma_\theta$ surface, the potential vorticity is generally more homogeneous across the Gulf Stream, except for a tongue of higher values centered at station 5881, which, referring to Fig. 1a, appears to be in the anticyclonic portion of the Stream. If the total potential vorticity were shown rather than just $f \times E$, the values in the tongue would be reduced slightly and the values just to the left of the tongue would increase slightly on account of the anticyclonic and cyclonic shears, respectively. The cross-stream potential vorticity distribution would then appear more uniform.

b. *Section III*

Many features in Section III (64°30′W) are similar to those in Section I, so only a brief discussion is necessary to emphasize the major points. The acceleration potential field for this section is shown in Fig. 2a. The tight group of contours between stations 5916 and 5918 indicates the position of the Gulf Stream, with the flow strongest between σ_θ = 26.6 and 26.8, then decreasing with increasing sigma-theta. The strong cyclonic feature centered at station 5922 is probably a cold core ring.

The temperature (Fig. 2b) and oxygen (Fig. 2c) sections are also similar to those for Section I in many ways. The sharp cross-stream temperature gradient between stations 5916 and 5917 only extends down to the $27.1\sigma_\theta$ surface as in Section I. But the temperature difference across the Gulf Stream is less (only 4°C along 26.6 compared to 6°C in Section I) and a wider band of Slope Water ($\theta \sim 12$°C at 26.7) appears between stations 5913 and 5916. A strong Shelf–Slope front ($\Delta\theta$ = 4°C) is also apparent between stations 5912 and 5913. The oxygen section also shows a strong cross-stream gradient between stations 5916 and 5917 down to the $27.1\sigma_\theta$ surface. Below that, the oxygen distribution along density surfaces crossing the Gulf Stream is very uniform. To note one other interesting feature, the strong cyclonic ring observed in the acceleration potential section to be centered at station 5922 has only a very weak oxygen signal centered somewhat farther to the north. Possibly the original high-oxygen Slope Water core has mixed isopycnally with surrounding Sargasso Sea Water in the upper water column.

As in Section I, the potential vorticity (Fig. 2d) jumps from 200 to greater than 500 ($\times 10^{-14}$ cm^{-1} s^{-1}) just north of the Gulf Stream (between stations 5916 and 5917). This potential vorticity gradient is strongest between σ_θ = 26.6 and 26.85, below which it begins to weaken so that below the $27.3\sigma_\theta$ surface, there is virtually no difference across the Stream. It is interesting to note that there is not much of a potential vorticity gradient along the density surfaces in the vicinity of the cold core ring, which may explain the lack of water mass contrast between the Sargasso Sea and the ring.

c. *Section VII*

Section VII is in the eastern half of the GS '60 survey, extending along 56°30′W from 46°N to 33°N. From the gradient of acceleration potential (Fig. 3a), we see that the Gulf Stream crosses this section between stations 149 and 151 (40–39°N). It is possible that the Stream has weakened somewhat, since the acceleration potential gradient across the Stream appears lower. But it is difficult to determine this conclusively because the Stream crosses this section obliquely, creating the impression of a wider, weaker current (see Fig. 6). Nonetheless, the downstream signal of the Gulf Stream extends down to the $27.8\sigma_\theta$ surface. South of the Stream, the broad, weak currents flowing both east and west may be associated with the Gulf Stream recirculation with mesoscale activity imbedded.

As with the western sections, there is a temperature front associated with the Gulf Stream (see Fig. 3b), as evidenced by the outcropping density surfaces, but the exact temperature difference across the front is impossible to measure along shallow density surfaces because of this outcropping immediately north of the

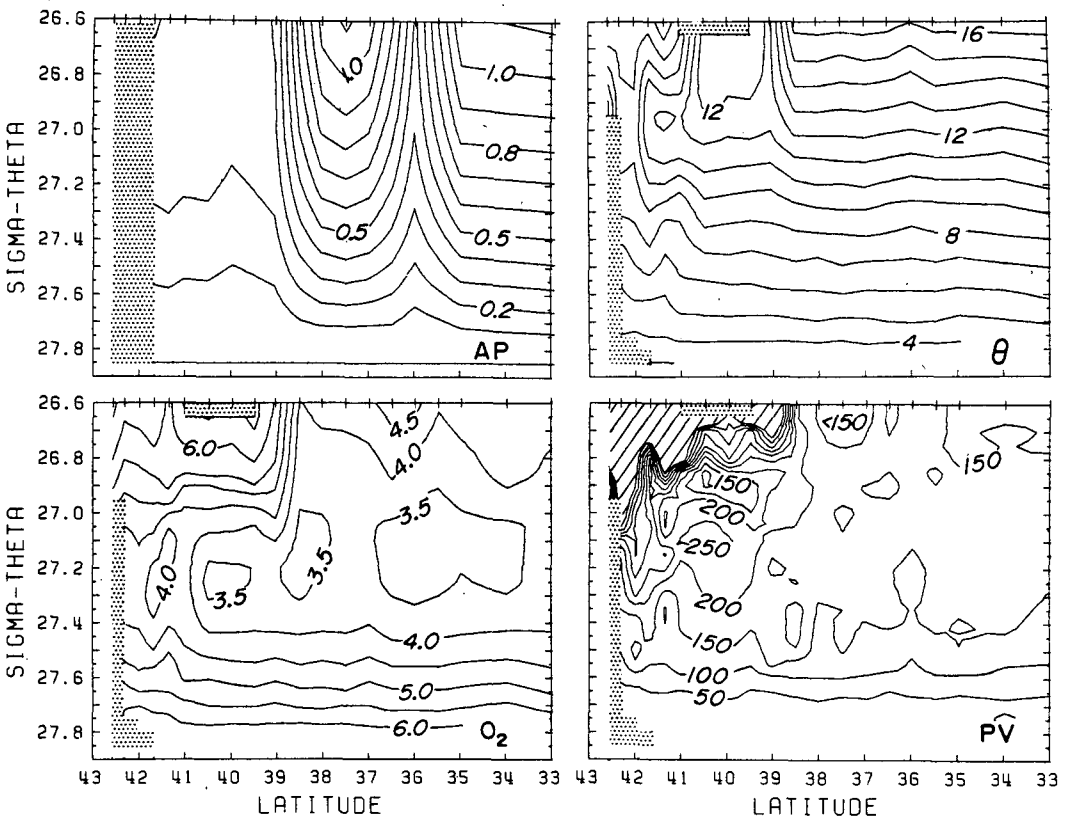

FIG. 2. As in Fig. 1 except for Section III of the GS '60 survey at 64°30'W, R.V. *Atlantis* 255 stations 5907–5926 (N to S).

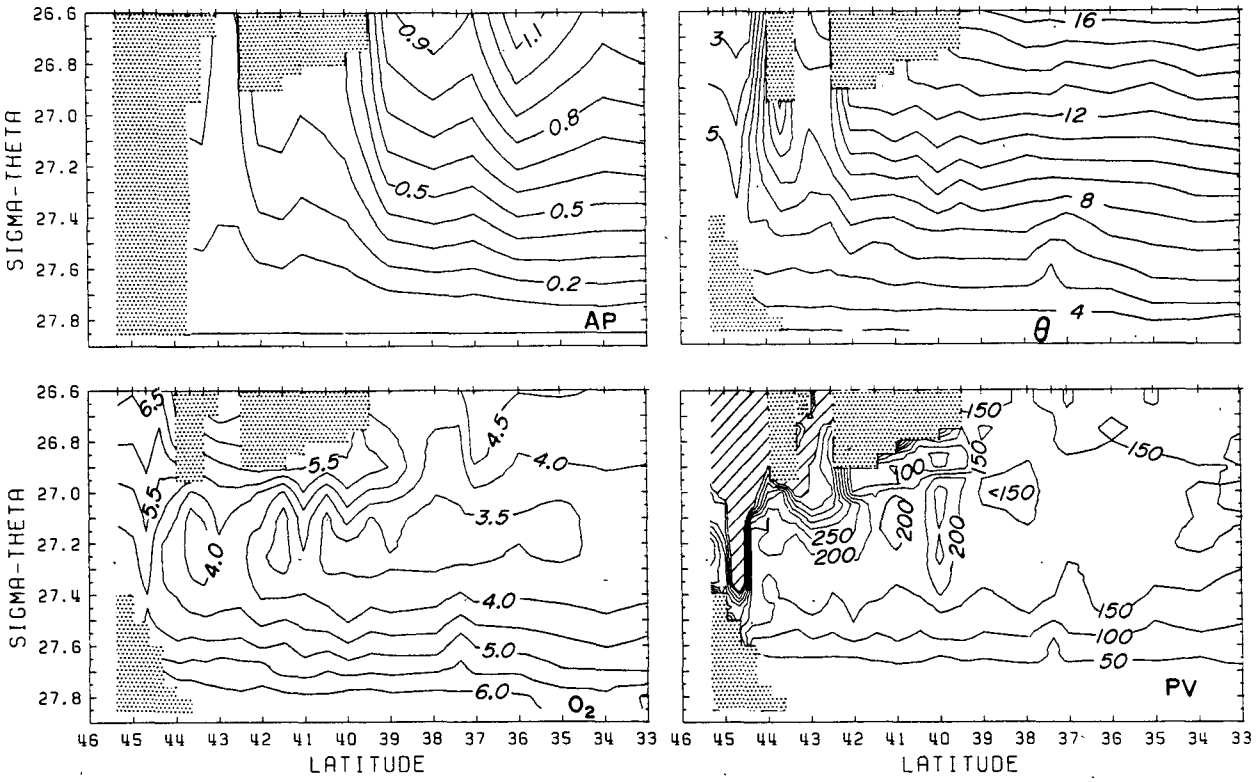

FIG. 3. As in Fig. 1 except for Section VII at 56°30'W, R.V. *Chain* 12 stations 136–151, 153–159 (N to S).

Stream. Below σ_θ = 26.9, a uniform cross-stream temperature distribution exists.

North of the Stream, there is a band of Slope Water between 41 and 42°N, then a sharp Shelf–Slope front ($\Delta\theta$ = 5°C) at 42°N, and then a third strong front ($\Delta\theta \sim$ 7°C) between 43 and 44°N. The very cold, fresh water north of 44°N is probably of coastal or Labrador Current origin. The downward slope of the isotherms south of the Stream between 12 and 6°C again indicates the presence of Mediterranean Water.

At first glance, the oxygen section (Fig. 3c) appears more complex than previous sections. But in fact, many features are the same. A strong oxygen gradient coincident with the Gulf Stream exists between stations 149 and 151. But the difference between values on either side of the Stream is less than in Section I (5.5–4.5 ml l^{-1} compared to 6.0–4.0 ml l^{-1} in Section I). Similarly, the potential vorticity field (Fig. 3d) under the outcropped region is more uniform than that for the same density surfaces in Section I.

d. Section VIII

The last and most easterly section we will examine is Section VIII, stretching from 45 to 33°N along 54°30′W. The sharpest acceleration potential gradient (Fig. 4a) is between stations 170 and 168, marking the position of the Gulf Stream. The relatively weak nature of this gradient, compared to Sections I and III, cannot be interpreted as a weakening of the current, again because of the oblique crossing (see Fig. 6).

Figure 4b shows that there is little temperature front between 40 and 39°N, however, an obvious indication of the Stream's position is the outcropping just north of the Stream. The Shelf–Slope front is found adjacent to the northern edge of the ventilated region. Below σ_θ = 26.85, there is thermal uniformity across the Stream and as far north as 43°20′N, where a strong subsurface front appears.

In Section VIII, there is still an oxygen gradient (Fig. 4c) associated with the maximum acceleration potential gradient. Despite difficulties in interpretation due to the large outcropped region, the coarse station spacing and the oblique angle of the Gulf Stream, the oxygen difference across the Stream appears to be slightly less than in the western sections. While there still seems to be a significant difference in the potential-vorticity distribution (Fig. 4d) across the Stream from σ_θ = 26.8 to σ_θ = 26.9, below that level, the homogeneity of the potential vorticity distribution across the Stream is striking.

Considering the above observations, we might first ask, what role does the Gulf Stream play in distributing water properties in this region, particularly dissolved oxygen? If there were no Gulf Stream at all between the source of high-oxygen waters in the north (seen

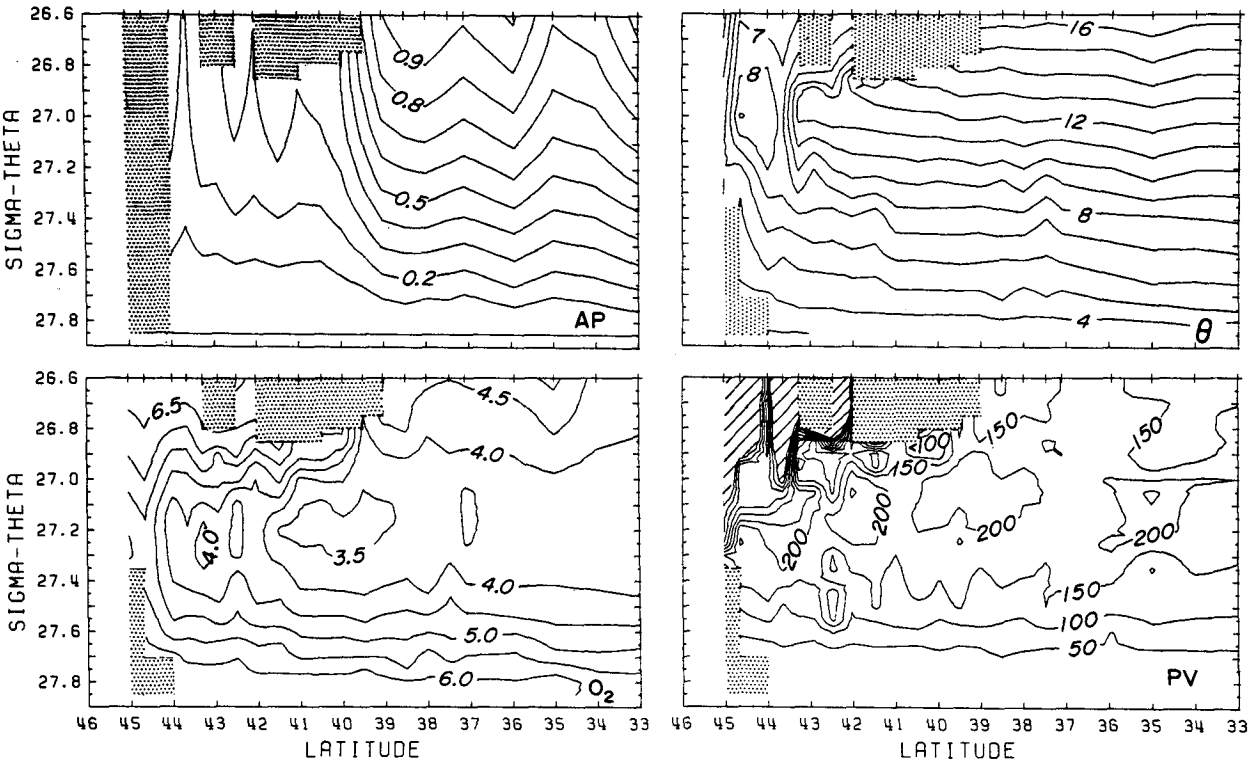

FIG. 4. As in Fig. 1 except for Section VIII at 54°30′W, R.V. *Chain* 12 stations 182–181, 179–160 (N to S).

in Figs. 3c and 4c north of 44°N down to σ_θ = 27.4) and the moderately low-oxygen waters of the Sargasso Sea, we would expect to see a gentle decrease in oxygen from north to south along isopycnal surfaces indicating the dominance of eddy diffusive processes. In fact, the sections described above support the existence of this type of regime below the 27.1σ_θ surface (in Sections I and III; shallower in Sections VII and VIII). The uniformity of the water properties below the 27.1σ_θ surface in the vicinity of the Gulf Stream indicates to us that Sargasso Sea Water and Slope Water are being effectively exchanged here. Furthermore, based on the uniformity of the potential vorticity fields, there is no dynamical constraint on the cross-stream exchange at this level. This is what we call the "blending" region.

On the other hand, we interpret the large cross-stream oxygen gradients above the 27.1σ_θ surface as evidence that the Gulf Stream is acting like a barrier here, prohibiting free isopycnal exchange between neighboring water masses. In accordance with this idea, the potential vorticity shows an abrupt jump across the Gulf Stream at these levels, imposing a severe dynamical constraint on cross-stream exchanges. Although our measure of the potential vorticity does not reflect contributions from the relative vorticity, which are important in the upper Gulf Stream, the simple difference in potential vorticity on either side of the Stream indicates an effective barrier to cross-stream flow as long as water parcels conserve potential vorticity.

West of 60°W, the barrier is very strong, based on the oxygen difference across the Stream above σ_θ = 27.1. East of that meridian, the outcropping density surfaces provide a very effective material boundary, but only down to the 26.9σ_θ surface. Below that level, the oxygen contrast across the Stream is weaker than in the west, which may signal a weakening of the Gulf Stream "barrier."

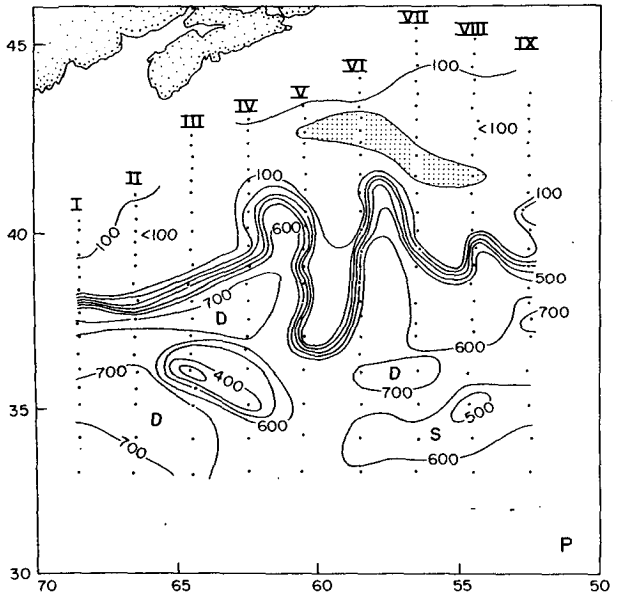

FIG. 5. Depth of the surface where σ_θ = 26.8, in meters. Sections are indicated by Roman numerals. Stippled areas indicate sea surface outcrops. D and S refer to deep and shallow, respectively.

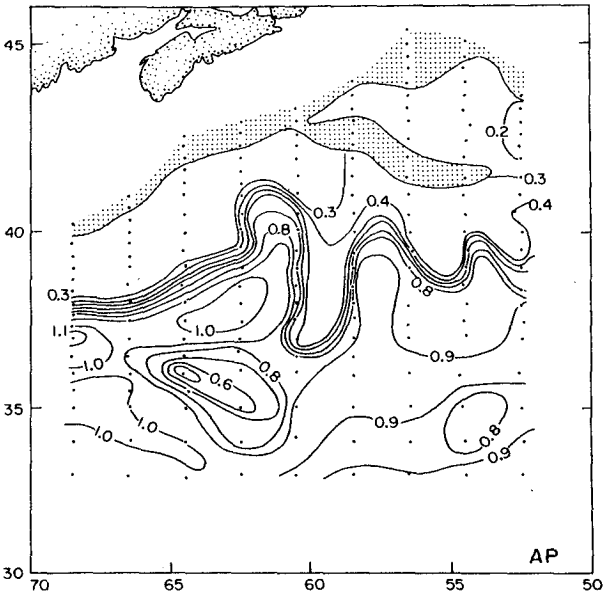

FIG. 6. Acceleration potential for the surface where σ_θ = 26.8, referenced to the surface where σ_θ = 27.85, in 0.1 dynamic meter intervals. Stipple indicates outcropping at the sea surface or bottom σ_θ less than 27.85.

After suggesting this concept of the Stream as a barrier to cross-stream exchange, we might next ask, exactly how opaque is the Gulf Stream? To answer this question, we have estimated the cross-frontal flux of oxygen in relation to the other oxygen fluxes in the region south of the Gulf Stream. The σ_θ = 26.8 density surface has a well-defined transition in oxygen all along the front, making it possible for us then to estimate a cross-frontal eddy diffusivity associated with the oxygen flux.

4. Oxygen fluxes

As we have noted above, the discontinuity of temperature, oxygen, and particularly potential vorticity across the cyclonic side of the Gulf Stream suggests that it is a strong barrier to cross-stream exchange. In Fig. 7, we have contoured the oxygen distribution on the σ_θ = 26.8 surface. For calculating the oxygen fluxes, we have isolated a pillbox-shaped layer 1 cm thick centered on the 26.8σ_θ surface. The box is bounded by Section I in the west, Section IX in the east, an east–west section at 33°N, and by the dynamical path of the Gulf Stream, defined by the 0.4 dynamic meter contour of acceleration potential (see Fig. 6), across which there is no transport. The approximate dimensions of this region are 1500 km in the streamwise direction and 500 km in the

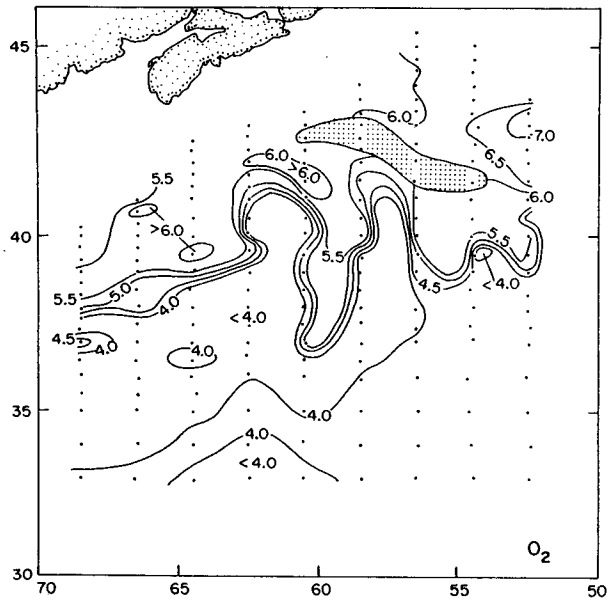

FIG. 7. Dissolved oxygen on the surface where $\sigma_\theta = 26.8$ in 0.5 ml l^{-1} intervals. Stippling as in Fig. 5.

meridional direction. By continuity, there can be no net mass flux out of this box. Because the acceleration potential and oxygen fields are given, we can estimate directly the advective fluxes through the meridional and southern boundaries.

We can further estimate contributions to the oxygen balance by Gulf Stream rings, diapycnal fluxes and biological uptake. We can then set bounds on the cross-stream diffusive flux of oxygen from the Slope Water.

We begin by integrating directly the advective fluxes through the bounding sections.

a. Section I

The oxygen influx in the Gulf Stream between the 0.4 and 0.8 dynamic meter acceleration potential contours has been integrated directly to be 16.5 $\times$ 10^5 ml s^{-1}, corresponding to a mean oxygen concentration of 3.7 ml l^{-1}. The remainder of the section to the south adds 4.6 $\times$ 10^5 ml s^{-1}, for a total inflow of 21.1 $\times$ 10^5 ml s^{-1}.

b. Section IX

The total flux out of the box through this section is 23.9 $\times$ 10^5 ml s^{-1}, of which 18.7 $\times$ 10^5 ml s^{-1} is provided by the Stream ($\bar{O}_2$ = 4.3 ml l^{-1} between 0.4 and 0.8 dynamic meter contours).

c. Southern section

The southwestward recirculation of the Gulf Stream waters leads to a small outward flux of 1.0 $\times$ 10^5 ml s^{-1}.

d. Gulf Stream rings

The flux by Gulf Stream rings is readily estimated. Assuming 10 rings form per year (Lai and Richardson, 1977), five of each kind so that there is no mass flow, and assuming the cold core rings are completely dissipated in the box, we obtain

$$(5 \text{ CCR yr}^{-1}) \times (50 \text{ km})^2 \times (\pi) \times (5.5 \text{ ml l}^{-1}) \times (1 \text{ cm}) - (5 \text{ WCR yr}^{-1}) \times (50 \text{ km})^2 \times (\pi) \times (4.0 \text{ ml l}^{-1}) \times (1 \text{ cm}) = 1.9 \times 10^4 \text{ ml s}^{-1}.$$

e. Biological uptake

The biological uptake throughout the region, using Jenkins's (1980) rate of 0.08 ml l^{-1} yr^{-1} at the depth corresponding to this σ_θ surface is about 1.5 $\times$ 10^4 ml s^{-1}.

f. Diapycnal flux

The diapycnal flux of oxygen is insignificant. The net vertical flux is simply

$$O_2 \text{ flux} = K_z \frac{\partial^2 O_2}{\partial z^2} \times (\text{volume of box}).$$

Assuming K_z = 1 cm^2 s^{-1} as an upper bound on the vertical diffusivity in the main thermocline, and $\partial^2 O_2/\partial z^2$ = 5 $\pm$ 2 ($\times 10^{-10}$ ml l^{-1} cm^{-2}) (averaged over many vertical profiles of oxygen in the Sargasso Sea), we obtain an oxygen input for a one cm thick layer to be 3 $\pm$ 1 ($\times 10^3$ ml s^{-1}), or less than 1% of the major fluxes. This is not a new or surprising result. Jenkins (1980) showed in some detail that simple vertical flux balances do not work.

The sum of these six terms is -3.7×10^5 ml s^{-1}, which should be balanced by a diffusive flux of oxygen across the Gulf Stream front into the region. This result is only meant to be an estimate, for which a detailed error analysis is difficult. We believe the flux estimate to within $\pm$50% based on the following sources of uncertainty: $\pm$0.1 ml l^{-1} in the mean oxygen values in the Gulf Stream; $\pm$25% in the fluxes through the meridional sections south of the Gulf Stream due to eddy variability; $\pm$2 Gulf Stream rings per year; and $\pm$25% in the oxygen consumption rate. In addition, a superimposed eastward barotropic flow field in the Gulf Stream of 0.10 m s^{-1} in the west and 0.15 m s^{-1} in the east would make the net oxygen flux only 27% larger, or -4.7×10^5 ml s^{-1}. So at least we are confident that the sign of this flux is correct.

It is of interest to compare this with what one might expect from conventional estimates of cross-stream eddy fluxes. We can use the computed oxygen divergence in our box to estimate the eddy diffusivity for steady-state balance to apply. Assuming an oxygen difference of 1.5 ml l^{-1} across the Stream on this

density surface, and a radius of deformation of 15 km, characteristic of eddy processes in the cyclonic shear zone (based on many XBT observations in the Stream at this level), we have

$$K_H \times (1.5 \text{ ml l}^{-1}) \times (15 \text{ km})^{-1} \times (1500 \text{ km}) \times (1 \text{ cm}) = 3.7 \times 10^5 \text{ ml s}^{-1},$$

or $K_H = 2.5 \times 10^6$ cm^2 s^{-1}. For comparison, Schmitt and Georgi (1982) have estimated the horizontal eddy diffusivity in the North Atlantic Current front to be 0.5–1.0 ($\times 10^5$ cm^2 s^{-1}), applicable for scales on the order of km's. On the scale of 100 km, Georgi and Schmitt (1983) estimate eddy diffusivities on the order of 10^7 cm^2 s^{-1}. It was counter-intuitive to us to find that double-diffusive processes can carry the entire burden of cross-frontal oxygen flux. We had expected ring formation to be the primary mechanism.

5. Summary

In this study we have used the Gulf Stream '60 hydrographic survey to examine the distributions of heat, oxygen and potential vorticity as a function of density and their relationship to the position of the Gulf Stream. Our objective has been to use these tracers to seek evidence for the Gulf Stream as a large-scale homogenizer on the one hand, and as a dynamical barrier to cross-stream exchange on the other. In a highly turbulent current one might expect these fields to become substantially uniform. In fact, however, we find the gradients of temperature, oxygen and potential vorticity to be very large, and to within the resolution of the hydrographic data, coincident with the cyclonic edge of the Gulf Stream. The sharpness of this water mass boundary all along the baroclinic Gulf Stream ($\sigma_\theta < 26.9$–27.1) for over 2000 km is testimony to its stability and robustness.

Although the large gradients indicate high impedance to cross-stream mixing there is of course some exchange taking place. This is observable in the form of pronounced interleaving of opposing water masses along the edge of the current. Using a simple control volume comprised of the Gulf Stream and parts of the recirculation system to the south we were able to estimate the cross-frontal flux of oxygen into the current from the Slope Waters. This translates into an eddy diffusivity of 2.5×10^6 cm^2 s^{-1} for scales appropriate for the cyclonic edge of the Stream, aproximately 15 km. This is quite consistent with the estimates of Schmitt and Georgi (1982) and Georgi and Schmitt (1983) of lateral diffusivity induced by double-diffusive processes.

One cannot discern from such a box model the nature of the processes responsible for these fluxes. Besides double-diffusive processes, up- and downwelling may force cross-frontal exchange, evidence for which may be shingle formation at the surface. A direct approach to the estimation of these fluxes is needed. A surprising result from this box model study was the small contribution to the oxygen balances played by warm and cold core ring formation.

The deep waters of the Gulf Stream show very little property contrast across the path of the Stream. Whereas the dynamical front is still well defined, all three tracers are very uniform. There is only a very weak north–south gradient between the cold high-oxygen waters along the continental escarpment and the more saline waters in the center of the North Atlantic subtropical gyre. In these deep waters, the energetic eddy field, induced by the meandering current, dominates and effectively homogenizes the tracer fields.

Acknowledgments. We thank a reviewer of an earlier version of this paper for a constructive and valuable critique. This work was supported by NSF Grant OCE-81-11498.

REFERENCES

Barba, R. C., 1978: A re-examination of the Gulf Stream '60 experiment. M.S. thesis, University of Rhode Island, Kingston, RI.

Buscaglia, J. L., 1971: On the circulation of the Intermediate Water in the southwestern Atlantic Ocean. *J. Mar. Res.*, **29**, 245–255.

Fofonoff, N. P., 1962: Dynamics of ocean currents. *The Sea: Ideas and Observations on Progress in the Study of the Seas*, Vol. 1: *Physical Oceanography*, M. N. Hill, Ed., Wiley–Interscience, 323–395.

Fuglister, F. C., 1963: Gulf Stream '60. *Progress in Oceanography*, Vol. 1, Pergamon, 265–273.

Georgi, D. T., and R. W. Schmitt, 1983: Fine and microstructure on a hydrographic section from the Azores to the Flemish Cap. *J. Phys. Oceanogr.*, **13**, 632–647.

Jenkins, W. J., 1980: Tritium and ^{3}He the Sargasso Sea. *J. Mar. Res.*, **38**, 533–569.

Lai, D. Y., and P. L. Richardson, 1977: Distribution and movement of Gulf Stream rings. *J. Phys. Oceanogr.*, **7**, 670–683.

Montgomery, R. B., 1937: A suggested method for representing gradient flow in isentropic surfaces. *Bull. Amer. Meteor. Soc.*, **18**, 210–212.

Munk, W. H., 1950: On the wind-driven ocean circulation. *J. Meteor.*, **7**, 79–93.

Reid, J. L., Jr., 1965: Intermediate waters of the Pacific Ocean. *The Johns Hopkins Oceanographic Studies*, No. 2, 85 pp.

Rossby, C.-G., 1936: Dynamics of steady ocean currents in the light of experimental fluid mechanics. *Pap. Phys. Oceanogr. Meteor.*, 5:1, 43 pp.

Schmitt, R. W., and D. T. Georgi, 1982: Finestructure and microstructure in the North Atlantic Current. *J. Mar. Res.*, **40**, 659–705.

Shaw, P.-T., and H. T. Rossby, 1984: Towards a Lagrangian description of the Gulf Stream. *J. Phys. Oceanogr.*, **14**, 528–540.

Stommel, H., 1965: *The Gulf Stream: A Physical and Dynamical Description*. 2nd ed., University of California Press, 248 pp.

Tsuchiya, M., 1968: Upper Waters of the Intertropical Pacific. *The Johns Hopkins Oceanographic Studies*, No. 4, 50 pp.

Veronis, G., 1973: Model of world ocean circulation: I. Wind-driven, two layer. *J. Mar. Res.*, **31**, 228–288.